inter.noise 2000
The 29th International Congress and Exhibition on Noise Control Engineering
27-30 August 2000, Nice, FRANCE

I-INCE Classification: 7.6

COMBINED CFD/CAA METHOD FOR CENTRIFUGAL FAN SIMULATION

F. Périé*, J.C. Buell**

* MCube, 166 rue de la Roquette, 750011, Paris, France

** Acusim Software, 14395 Saratoga ave Suite 110, 95070, Saratoga CA, United States Of America

Tel.: 33 (0) 1 43 70 06 44 / Fax: 33 (0) 1 55 59 96 36 / Email: fred@mcube.fr

Keywords:
CFD, CAA, FAN, LES

ABSTRACT
A 140000 2D FE model is used to simulate a 44 blades centrifugal fan. The purpose of this paper is to evaluate and compare two different numerical approaches. One is a classical CFD solution involving an implicit FE solver, a fixed topology with a rotating reference frame and a turbulent model. The other solution involves an explicit FE solver, which accounts for topology changes and takes advantage of LES to simulate unsteady turbulent structures as well as aeroacoustic noises (CAA). Interest and limitations of both methods are analyzed. Also compared is the predicted noise to experimental results in the far field.

1 - INTRODUCTION

Computational fluid dynamics and aeroacoustics are challenging tasks when dealing with complex phenomena involved in a centrifugal blower. A non restrictive list of modeling difficulties include: change of topology due to blade passing, turbulent phenomena at the blade tip, unsteadiness of the flow involving small to large scales, acoustic contribution of turbulence, acoustic wave propagation, impedance of inlet and outlet boundaries, noise transmission to shroud... When addressing this problem, two fundamental questions arise:

- Is an average flow assumption relevant? If yes, is a fixed topology and steady state approach able to reproduce the flow field with a reasonable accuracy?
- When taking into account topology changes, does a transient approach provide better prediction of the flow and will it in addition describe accurately flow induced noises?

In this paper, we compare two rather different numerical approaches to the simulation of centrifugal blowers. The Implicit and Explicit modules of the Radioss CFD/CAA systems are here tested on an idealized 2D problem (Fig. 1). Despite the obvious 3D nature of the flow in real centrifugal blowers, specially when aeroacoustics is involved, a crude 2D approximation is used here for investigation and illustration purposes. Industrial 3D calculations are currently being conducted, which will be published in the near future.
The 44 blades wheel is rotating at 3 133 RPM. In the experimental set-up, the fan was blowing inside an INCE box, where the average pressure was measured and the noise was recorded at 2 meters away in front of the blower outlet. As the experimental value for the inlet flux was not available to the authors, it was estimated from other sources. An 11.3 m/s radial flux is imposed at the inlet ring and a zero static pressure is imposed at the outlet section for reference.

2 - NUMERICAL METHODS

2.1 - CFD approach

The classical CFD approach allows for simplifications of the problem by considering

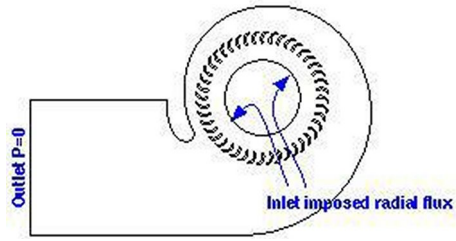

Figure 1: Schematic description of the problem.

- a fixed topology of the rotating wheel
- centrifugal and Coriolis forces in the wheel region
- the air as incompressible
- turbulence as fully modeled by a RANS approach

The steady state solution is obtained by solving Navier-Stokes equations with the implicit module of the Radioss CFD system. The governing equations are:
Mass:

$$\nabla \cdot \mathbf{u} = 0 \tag{1a}$$

Momentum:

$$\rho \partial \mathbf{u}/\partial t + \rho \left(\mathbf{u} \cdot \nabla\right) \mathbf{u} - \nabla \tau + \nabla p = 0 \tag{1b}$$

where bold characters denoting vector quantities and the operator ∇ stands for $(\partial/\partial x, \partial/\partial y, \partial/\partial z)$, $\mathbf{u}$ the velocity vector, τ the shear stress tensor and p is the pressure
Above equations are solved using the Galerkin/Least-Squares finite element technology developed by Acusim software [1]; see [2] and references therein for in-depth description. Equations (1a) and (1b) are treated as a coupled system yielding substantially faster nonlinear convergence. Furthermore, the implicit module is structured and all the algorithms are designed specifically to perform on coarse-grain parallel machines using either Message Passing Interface (MPI) or SMP.
The turbulence behavior of the flow is modeled with the one-equation Spalart-Allmaras model; see [3] for details and definition.
In the proposed CFD approach, we consider two domains, one is in the laboratory reference frame, the other is calculated according to a rotating reference frame, i.e. centrifugal and Coriolis forces are added to eq. (1b):

$$\rho \partial \mathbf{u}/\partial t + \rho \left(\mathbf{u} \cdot \nabla\right) \mathbf{u} - \nabla \tau + \nabla p = -\rho \Omega \wedge \Omega \wedge (\mathbf{x} - \mathbf{x}_0\ ) - 2\rho \Omega \wedge \mathbf{u} \tag{1c}$$

where $\mathbf{x}$ is the nodal coordinate vector; $\mathbf{x}_0$ is the center of rotation.
This assumption obviously neglects the local transient nature of the flow and gives privilege to a specific relative position of the blades with respect to the volute. This is thought to be valid for centrifugal blowers, due to the high number of blades and the short turbulent mixing zone in their wake. Furthermore, the fixed topology assumption obviously makes sense only within a steady state framework. This means that unlike the LES approach described hereafter, the turbulent model is here supposed to be able to segregate the flow into its mean component which is solved, and the average fluctuations that are modeled.

2.2 - CAA approach

The method of approach taken in this paper for computational aeroacoustics attempts to take into account several physics in a single simulation:

- change of topology due to blade passing,
- microscopic turbulent scales,
- unsteadiness of the flow involving macroscopic scales at the blade tip,
- acoustic contribution of turbulence,

- acoustic wave propagation including impedance of boundaries,
- noise transmission to structures (although this issue can be tackled by the code, it is not in the scope of this paper)

The transient aeroacoustic simulation is performed with the explicit module of Radioss CFD/CAA developed by Mecalog [4]. Its formulation is *Arbitrary Lagrangian Eulerian* (ALE) [5]: each point in space having a grid velocity $\mathbf{w}$ describing its arbitrary movement in the same time as the usual material velocity $\mathbf{u}$. Conservation laws may be written as:
Mass:

$$\partial\rho/\partial t + ((\mathbf{u}-\mathbf{w})\cdot\nabla)\,\rho + \rho\nabla\cdot\mathbf{u} = 0 \tag{2a}$$

Momentum:

$$\rho\partial\mathbf{u}/\partial t + \rho\,((\mathbf{u}-\mathbf{w})\cdot\nabla)\,\mathbf{u} - \nabla\tau + \nabla p = 0 \tag{2b}$$

Energy:

$$\partial\rho e/\partial t + ((\mathbf{u}-\mathbf{w})\cdot\nabla)\,\rho e + (\rho e + p)\,\nabla\cdot\mathbf{u} = 0 \tag{2c}$$

Note that for $\mathbf{u}$=$\mathbf{w}$, equations (2a)-(2c) reduce to Lagrangian description, while for $\mathbf{w}$= 0, they describe the Eulerian case. As a consequence, a single formulation is able to describe the evolution of physical variables in the laboratory reference frame and in a grid with any arbitrary movement (e.g. rotation).
The spatial integration is achieved with a Finite Element formulation with a *Streamline Upwind Petrov Galerkin* (SUPG) integration scheme [6]. The time integration is performed with an explicit centered integration scheme, whose stability is governed by Courant's condition:

$$dt \leq \min\left(\Delta/\left(c + \|\mathbf{u}\|\right)\right) \tag{3}$$

with Δ being the characteristic element size and c speed of sound.
This results in very small time steps that together with SUPG provide minimal numerical diffusion and enough accuracy to capture and to convey the resolved vortices. In the *Large Eddy Simulation* (LES) [7], turbulent structures smaller than what can be resolved by the grid ($\sim 6\Delta$) are filtered out by the spatial discretization and must be taken into account by a so-called Sub-Grid Scale model (here the Smagorinsky model).
The proposed method does not pretend to resolve turbulence near walls. A special treatment assumes a logarithmic profile and computes the turbulent viscosity at the boundary layer as if all turbulent structures were unresolved there. A special care is also taken for sound absorption due to the near wall turbulence [8].
LES requires however very small elements and a simulated physical duration long enough to capture a large number of flow realizations and to acquire enough samples for noise analysis. This means intensive computing. In the current version of the code, a fully parallel algorithm is implemented using a shared memory approach.
Note that by nature, the compressible nature of equations (2a)-(2c) takes into account acoustic wave propagation within the computational domain. Here a linearized compressibility is used instead of a perfect gas law. This assumption is equivalent to an isothermal assumption and allows to neglect equation (2c) and to neglect the advection term in equation (2b).
The outlet impedance is modeled by the linearized Euler equation of Bayliss and Turkell's [9]:

$$\partial p/\partial t = \rho c\partial u_n/\partial t - u_n\nabla\cdot(\mathbf{u} - u_n\mathbf{n}) + c/2l_c\,(P_\infty - p) \tag{4}$$

with u_n the velocity normal at the boundary, and $\mathbf{n}$ the local normal vector.
The first term is the Sommerfeld impedance and the last one is a relaxation term toward the imposed average value P_∞; (this is equivalent to a high pass filter). Note that a Fourier analysis of (4) shows that these two terms approximate the radiation impedance of a piston whose radius is roughly l_c.
The coupling between the rotating grid and the fixed grid achieved with a simple finite element interpolation scheme.

3 - MODEL

A 140000 FE model (Fig. 2) is built for both the explicit and the implicit solvers. In order to capture the turbulent features when using LES, a very fine unstructured mesh is used in the vicinity of the blades and neck. The mesh size ranges from 0.4 mm near the blades and downstream to 7 mm in the outlet channel,

the latter allowing for propagation of acoustic waves up to 8 000 Hz (6 elements per wave length). A 11.3 m/s radial velocity is imposed on the inlet ring whereas a zero reference pressure is applied at the outlet (in the explicit calculation, the silent boundary capability imposes the average static pressure as in eq. (4) with l_c=50 mm).

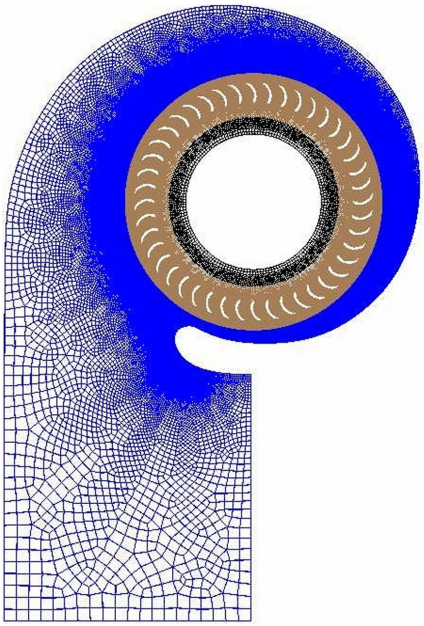

Figure 2(a): General view of the model.

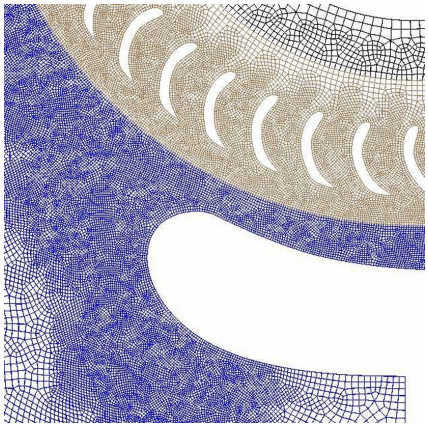

Figure 2(b): Detailed view of the mesh.

4 - NUMERICAL RESULT

4.1 - Flow results

The implicit and explicit solutions exhibit some similarities and also some differences. Fig 3a and 3b show that the pressure and velocity fields are globally similar except in three regions:

- Between the volute neck and the rotating wheel, where higher pressures can be observed in the explicit calculation as well as "low pressures bubbles" corresponding to vortices whose spacing (12 mm) is close to the blade spacing (Fig. 4).
- Close to the volute neck, the pressure gradient is much lower in the implicit solution, where a "quiet" region can be observed.
- In the wake of the volute neck, where vortex shedding happens in the explicit calculation, whereas the implicit solver gives a steady solution.

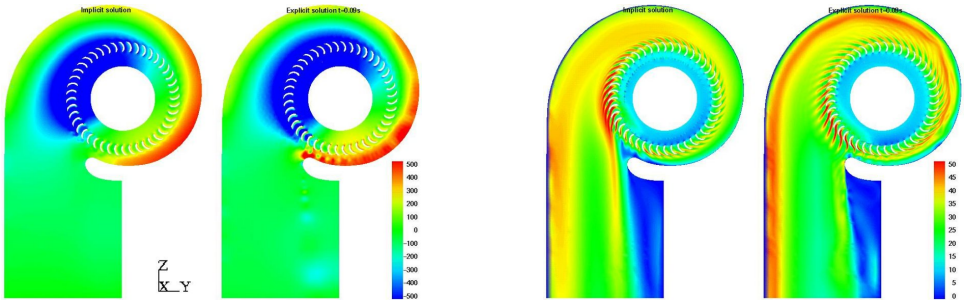

(a): Pressure (Pa). **(b):** Velocity (m/s).

Figure 3: Comparison of implicit and explicit fields.

Both simulations exhibit two regions of higher velocities in the outlet channel, namely the outer wall of the volute and the wake of the neck. However the flux near the neck is lower in the explicit calculation

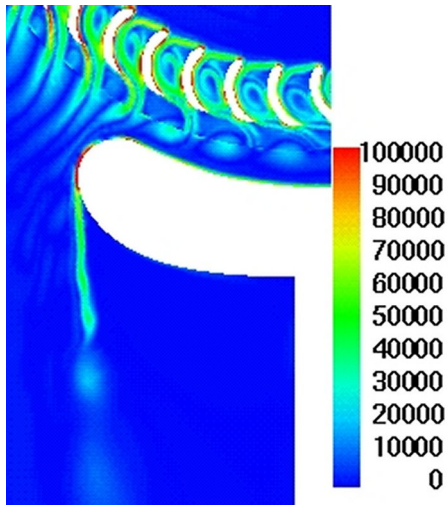

Figure 4: Detailed view of vorticity contours in the neck vicinity.

and higher near the outer wall. In fact, the flow appears more "centrifugal" in the explicit calculation whereas it is more "tangential" in the implicit case, specially in the neck region.
The comparison of the total pressure jump from inlet to outlet can be compared with the experimental value (Table 1). An error of more than 25 % can be observed. This means that the flux imposed at the inlet of the model has been overestimated. Furthermore the flux was supposed uniform round the inlet ring. This assumption is probably unrealistic as the high pressure near the neck may cause upstream recirculations in real 3D configuration. Further calculations will be conducted to remedy this problem.
The explicit calculation leads to lower reaction forces for a higher pressure jump (better efficiency), which is probably due to an overestimation of the turbulent viscous term in the implicit approach.

Axis reaction loads	Implicit	Explicit	Experimental
x-Moment (N.m)	-0.654	-0.586 +/-0.003	N/A
y-Force (N)	-1.798	-0.768 +/-0.1	N/A
z-Force (N)	4.7	3.86 +/-0.04	N/A
Average ΔP_{total} (Pa)	408	454	623

Table 1: Comparison of reaction loads for implicit and explicit solutions.

	Elapsed Time (h)	Steps	Final time
Implicit	7	64	converged steady state
Explicit	45	91 800	0.095 s

Table 2: Elapsed time on a dedicated SGI O2000 (16xR10k 190 MHz) and number of steps/iterations.

4.2 - Noise results

During the simulation of 0.095 second of physical time, signals at all the nodes of the outlet section are recorded using a 33.3 kHz sampling frequency with a low-pass filter to avoid frequency folding around Nyquist frequency. Fourier transforms are then applied to these data to analyze the results in the frequency domain.
Acoustic convergence is verified on spectra and levels for different blocks of the signal: It is obtained after roughly 0.05 seconds. Sound pressure radiation outside the computational domain is then evaluated. For this purpose, two methods are proposed: The first one is valid for *harmonic noise* sources: integration is performed over the outlet surface by taking into account each node magnitude and phase spectra as if it was a monopolar source term radiating over 2π radians (Rayleigh radiation):

$$\hat{p}\left(f\right) = j\rho f \int\int \hat{v}_n\left(f\right) \frac{e^{-jkr}}{r} dS \tag{5}$$

The second one considers all the nodes as not coherent monopolar sources and the integration is performed without considering phases. This assumption is only valid for non correlated noise sources:

$$\hat{p}\,(f) = \rho f \sqrt{\int\int \hat{v}_n^2\,(f)\,dS} \tag{6}$$

Eq. (5) should be considered for tonal noises and eq. (6) for broad band noises. In the experiment, the blower was mounted on an INCE box to control the fan load and sound was recorded on DAT tape at 2 m in front of the blower outlet [10]. Both experimental and numerical noise are compared in terms of sound pressure levels (Table 3) and spectra (Fig. 5a and 5b).

	Numerical		Experimental
Freq. range	Rayleigh	Decorrelated	
[100-6 000] Hz	73	83	65
[500-6 000] Hz	64	71	63

Table 3: Comparison of experimental and simulation SPL (dBA).

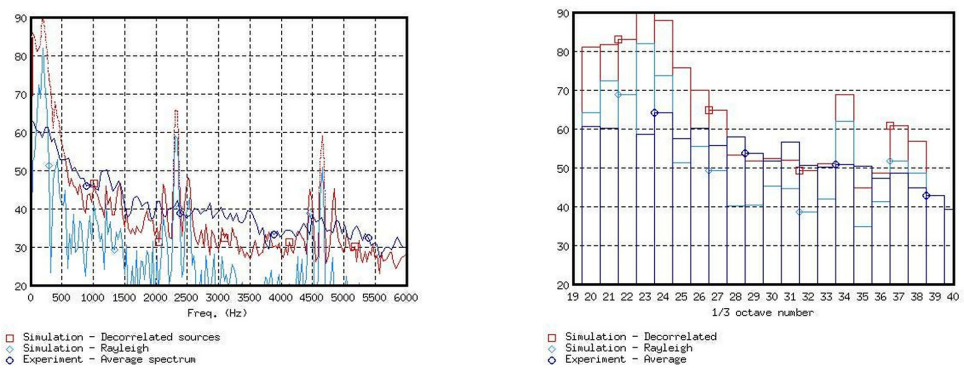

(a): Short band spectrum (res. ∼30 Hz).

(b): 1/3 octave.

Figure 5: Comparison of SPL at 2 m from fan orifice (dB ref. 2 10^{-5} Pa).

Simulation results exhibit several tonal noises at 195, 2 300 and 4 600 Hz. The blade passing frequency 2 300 Hz (BPF) and its harmonics emerge significantly (58 dB and 50 dB). They radiate as a superimposition of monopole and a dipole as shown by Fig. 6, which shows the modal deformation of the outlet section.

Figure 6: Modal deformation of the outlet opening for blade passing frequency (2 298 Hz).

On the other hand, the experimental spectrum has only two emerging peaks, 62 dB around 230 Hz and 50 dB at 1 150 Hz, the latter being half of BPF and close to the transverse eigen mode of the outlet channel, which is not accounted for in formula 4 and 5, whereas the BPF itself is absent. The experimental signal is dominated by broad band noises, for which the numerical prediction of eq. (6) is more accurate (3 to 8 dB differences).
The observed discrepancies can be explained by approximations made in the model:

- The imposed flux was overestimated and the resulting jets coming out of the blower wheel are strong enough to interact with the neck of the volute.
- The uniform inlet flux due to the 2D assumption increases the previous phenomenon
- The 2D assumption prevents the turbulent mixing occurring in the third direction
- The cavity modes in the third direction are not taken into account.
- The structure is assumed rigid so that the noise absorbed in the plastic casing is neglected.

A better modeling of the inlet may greatly improve the first two points.

5 - CONCLUSION

The flow obtained by both the implicit and the explicit solution are compared in terms. The global behavior is similar, although some differences can be observed close to the blower wheel. The reaction moment and the pressure jump through the fan are different by only 12 %. This provides us with some confidence that an implicit and steady state solution is probably good enough to evaluate the fan performance. More work needs to be done to fully validate the approach on a 3D case, e.g. by comparing numerical and experimental performance curves.
The second comparison is between the CAA noise results and the test data, in spite of the many recognized inconsistencies between the physical and numerical test. Correlation of measured and predicted broad band noises appear satisfactory. However, the numerical predictions exhibit pronounced tonal noises absent from the experiment. Improving the inlet conditions should improve this point. Future work will focus on the inlet modeling and thus the flow paths close to the volute of the neck; this should improve significantly the noise results.

ACKNOWLEDGEMENTS

The authors would like to thank Ken Jacobson of SGI for loaning us the system used for the simulations.

REFERENCES

1. **Acusim software**, *ACUSOLVE Command Reference Manual version 1.3*, 1999
2. **T.J.R. Hughes**, Recent Progress in the Development and Understanding of SUPG Methods with Special Reference to the Compressible Euler and, *Int. J. Numer. Methods Fluids*, Vol. 7, pp. 1261-1275, 1987
3. **P.R. Spalart and S.R. Allmaras**, A One-Equation Turbulence Model for Aerodynamic Flows, In *AIAA*, 1992
4. **Mecalog**, *RADIOSS CFD user manual version 3.2*, 1999
5. **J. Donea**, *Arbitrary Lagrangian-Eulerian Finite Elements Methods*, Computational Methods in Transient Analysis, 1983
6. **A.N. Brooks and T.J.R. Hughes**, Streamline Upwind/Petrov-Galerkin Formulations for Convection Dominated Flows with particular Emphasis on the, *Computer Methods in Applied Mechanics and Engineering* , Vol. 32, 1982
7. **P. Sagaut**, *Simulation des grosses structures*, Ecole de Printemps de mécanique des fluides numériques, 1997
8. **M.S. Howe**, *Acoustics of Fluid-Structure Interactions*, Cambridge Monographs on Mechanics, pp. 318-326, 1998
9. **A. Bayliss and E. Turkell**, Outflow Boundary Conditions for Fluid Dynamics, *SIAM J. Sci. Stat. Comput.*, Vol. 3(2), 1982
10. **Morris Hsi and Fred. Périé** , Acoustic Performance Analysis of an Air Handling System, In *SAE Noise and Vibration Conference*, pp. 65-75, 1997